Earth and Planetary Science Letters 440 (2016) 1–11

Contents lists available at ScienceDirect

Earth and Planetary Science Letters

www.elsevier.com/locate/epsl

Influence of vegetation type and site-to-site variability on soil carbonate clumped isotope records, Andean piedmont of Central Argentina (32–34°S)

Mallory C. Ringham [a,*], Gregory D. Hoke [a], Katharine W. Huntington [b], Julieta N. Aranibar [c]

[a] Earth Sciences, Syracuse University, Syracuse, NY, 13244, United States
[b] Earth and Space Sciences, University of Washington, Seattle, Washington, United States
[c] Instituto Argentino de Nivologia, Glaciologia y Ciencias Ambientales, CCT-Mendoza, 5500 Mendoza, Argentina

ARTICLE INFO

Article history:
Received 3 September 2015
Received in revised form 31 January 2016
Accepted 2 February 2016
Available online 11 February 2016
Editor: D. Vance

Keywords:
pedogenic carbonate
clumped isotope thermometry
stable isotopes
temperature proxy
central Andean piedmont
paleoclimate

ABSTRACT

The clumped isotope geothermometer estimates the formation temperature ($T(\Delta_{47})$) of carbonates and has great potential to enhance the extraction of environmental data from pedogenic (soil) carbonate in the geologic record. However, the influence of vegetation type and site-specific conditions on carbonate formation processes and $T(\Delta_{47})$ records remains poorly understood. This study examines the potential for variability in $T(\Delta_{47})$ data between nearby, same elevation sites with different C_3/C_4 biomass. Pedogenic carbonates (undercoatings and nodules) were collected from five modern soil pits in the semi-arid eastern Andean piedmont of Argentina under a summer precipitation regime. Three pits were instrumented with temperature and moisture sensors to 1 m depth, and a fourth was instrumented with additional soil CO_2 and atmospheric (temperature, relative humidity, insolation, and rainfall) sensors. $T(\Delta_{47})$ values (mean: 30 ± 6 °C ($\pm$1SE)) are invariant with depth and are statistically indistinguishable between the four instrumented sites, though a 10 °C difference between our $T(\Delta_{47})$ values and those of a nearby Peters et al. (2013, EPSL) study suggests the potential for significant site-to-site variability, likely due to local soil hydrology. The results of this study suggest that deeper ($\geq$40 cm) $T(\Delta_{47})$ values are consistent with carbonate formation during the early part of soil drying immediately after large mid-summer rainstorms. Carbonate formation $\leq$ 40 cm depth may be biased to soil drying after small, frequent precipitation events occurring throughout the spring, summer, and fall months, averaging to shallow summer $T(\Delta_{47})$ values and resulting in a near-isothermal $T(\Delta_{47})$ profile.

1. Introduction

The development of low temperature geothermometers is important to researchers studying Earth surface processes, paleoaltimetry, and paleoclimate. The clumped isotope geothermometer allows for the determination of near-surface temperatures based on the relative degree of ^{13}C–^{18}O bonding in carbonates ($CaCO_3$). "Clumping" of these heavy isotopes varies inversely with temperature, providing an estimate of carbonate formation temperature ($T(\Delta_{47})$, where Δ_{47} refers to the abundance of ^{13}C–^{18}O bonds in CO_2 gas derived from carbonate in excess of a stochastic distribution) that is independent of bulk isotopic composition (Ghosh et al., 2006a; Eiler, 2007). Thus, clumped isotope thermometry solves the issue of two unknowns in conventional stable isotope analysis of carbonate, in which carbonate $\delta^{18}O$ depends on both the temperature of mineral formation and the oxygen isotopic composition of the soil water.

Early uses of clumped isotope geothermometry assumed that pedogenic carbonate formation temperatures reflect mean annual soil temperatures (MAST), with potential systematic errors due to seasonal biases (e.g. Ghosh et al., 2006b). Breecker et al. (2009) calculated a strong seasonal bias for carbonate formation during warm, drying episodes in the soil when soil pCO_2 is low. Several studies have found $T(\Delta_{47})$ to be far in excess of MAST (e.g. Passey et al., 2010; Quade et al., 2013; Hough et al., 2013) or to reflect a mixture of summer and fall temperatures depending on the timing of the wet season and snowmelt (Peters et al., 2013). Depth-resolved $T(\Delta_{47})$ data are reported in Passey et al. (2010), Quade et al. (2013), and Peters et al. (2013), and nearly all published $T(\Delta_{47})$ profiles are isothermal with depth. Quade et al. (2013) interpreted their $T(\Delta_{47})$ data as decreasing with depth, following the pattern

DOI of related article: http://dx.doi.org/10.1016/j.epsl.2016.02.033.
* Corresponding author.
E-mail address: mcringha@syr.edu (M.C. Ringham).

http://dx.doi.org/10.1016/j.epsl.2016.02.003
0012-821X/

for summer soil temperatures; however, with consideration of the typical 4–6 °C uncertainty in clumped isotope methods, these data appear to be isothermal. Peters et al. (2013) observed no systematic decrease in $T(\Delta_{47})$ with depth, which was consistent with typical fall soil temperatures. Together these data call into question our collective understanding of carbonate formation in the soil profile, such that summer biases for $T(\Delta_{47})$ are generally accepted, though $T(\Delta_{47})$ with depth and the timing of carbonate precipitation in soil require clarification.

This study examines the potential for variability of $T(\Delta_{47})$ data from soil carbonate nodules and undercoatings collected in the Andean piedmont of Argentina (32.5–34°S; Fig. 1) in order to better constrain the conditions that lead to carbonate precipitation and to improve interpretations of clumped isotope paleoenvironmental records. We simplified our investigation by (1) choosing sites in a summer-only precipitation regime, thereby limiting variability in seasonal soil drying, (2) varying C_4/C_3 biomass, which may bias seasonal soil moisture and CO_2 conditions during times of peak productivity, and (3) comparing same elevation nearby sites, as some studies show a strong correlation between $T(\Delta_{47})$ and elevation (Quade et al., 2013; Hough et al., 2013) while others do not (Peters et al., 2013). Our objectives are to explore the influence of environmental variables on the timing of pedogenic carbonate formation via *in-situ* monitoring of atmospheric conditions, soil temperature, soil moisture, soil gas CO_2 concentration, and vegetation type, and to determine the potential for site-to-site variability in resulting $T(\Delta_{47})$ values.

2. Background

2.1. Controls on pedogenic carbonate formation

Pedogenic carbonate forms over hundreds to thousands of years as filaments, root casts, nodules, clast undercoatings, or horizons in sub-humid to arid soils when the soil solution becomes supersaturated with calcite (Gile et al., 1966; Cerling and Quade, 1993). The carbonate formation reaction,

$$CaCO_{3(s)} + CO_{2_{(g)}} + H_2O \leftrightarrow Ca^{2+}_{(aq)} + 2HCO^{-}_{3_{(aq)}} \quad (1)$$

and its corresponding activity equation under aqueous conditions,

$$\alpha_{CaCO_3} = \frac{4m^3_{Ca^{2+}}}{pCO_2}\left(\frac{K_2}{K_1 K_{cal} K_{CO_2}}\right) \quad (2)$$

show that carbonate precipitation in soils may result from increasing soil temperature, decreasing soil gas pCO_2, or increasing Ca^{2+} or HCO_3^- concentration in solution (Breecker et al., 2009). In well-drained, arid climate soils, carbonate should form during periods of soil dewatering due to evaporation, root uptake, and decreasing pCO_2 (Huxman et al., 2004; Liu et al., 2002). Soil CO_2 is an admixture of atmospheric CO_2 and biologically respired CO_2. Typically, pedogenic carbonate $\delta^{13}C$ in a soil profile exhibits a positive shift near the surface reflecting a decrease in the respired component of soil CO_2 (Luo and Zhou, 2006; Cerling and Quade, 1993). $\delta^{18}O_{carbonate}$ depends on $\delta^{18}O_{soil\ water\ (SW)}$ and temperature-dependent fractionation during carbonate formation. In well-drained soils, $\delta^{18}O_{SW}$ is commonly assumed to reflect meteoric water, and is typically enriched near the surface by evaporation (e.g. Cerling and Quade, 1993). In equation (2), pCO_2 is the partial pressure of soil gas carbon dioxide, $m_{Ca^{2+}}$ is the soil solution calcium ion concentration (provided by rainwater and dissolution of Ca-bearing minerals in dust or soil parent material, e.g., Gile et al., 1966; Machette, 1985), and K values are temperature-sensitive equilibrium constants (Drever, 1982; Plummer and Busenberg, 1982). A value of alpha (α_{CaCO_3}) > 1 indicates precipitation of $CaCO_3$. This equation is valid for systems in thermodynamic equilibrium where activity ≈ concentration and soil water pH ≤ 9. Recent studies have suggested that isotopic equilibrium in carbonate formation is not always achieved (Gabitov et al., 2012) due to kinetic isotopic effects that may result in increased apparent $T(\Delta_{47})$ values (Guo, 2008). However, most studies of soils assume that pedogenic carbonate forms in isotopic equilibrium with soil CO_2 and soil water during drying episodes (Breecker et al., 2009; Cerling and Quade, 1993).

Recent studies have combined soil carbonate clumped isotope thermometry with *in-situ* soil monitoring to investigate how these factors affect carbonate formation and $T(\Delta_{47})$ records; most published data suggest a summer temperature bias in carbonate formation, but soil moisture balance may be more important. Quade et al. (2013) found that average $T(\Delta_{47})$ measurements of modern soil and paleosol carbonates from soils typically developed under summer rainfall seasonality reflected the hottest months of the year when the soil was dry, exceeding the mean annual air temperature (MAAT) by 10–15 °C. Passey et al. (2010) found that temperatures recorded by modern soil carbonates in temperate latitudes exceeded present-day MAST, plotting closely with average summer soil temperatures. Peters et al. (2013) investigated carbonate formation temperatures along an Andes elevation transect at ~33°S and found that average $T(\Delta_{47})$ values for carbonates collected above 2 km elevation reflect summer soil temperatures, while those below 2 km more closely reflect MAST. This transition coincides with a change in seasonality of precipitation. This study suggested that below 2 km, summer rainfall delays soil drying until fall, allowing carbonate formation later in the year to record cooler $T(\Delta_{47})$ values. Above 2 km, under winter precipitation, soil dries during the warmest months, allowing for carbonate formation with summer $T(\Delta_{47})$.

Few studies have investigated the behavior of $T(\Delta_{47})$ with depth. Quade et al. (2013) reported decreasing $T(\Delta_{47})$ with depth, attributed to summer soil temperatures intensified by radiative heating at the surface; however, these profiles do not vary with depth if considered with typical 4–6 °C uncertainties. Peters et al. (2013) reported isothermal profiles that could be attributed to soil heterogeneity or to higher frequency of carbonate formation at the surface than at depth, such that if carbonate formation at depth occurs rarely, in response to abnormally hot conditions, $T(\Delta_{47})$ will be more constant throughout the soil profile.

The type and amount of vegetation in a region may also influence the timing of carbonate formation because plants impact radiative heating at the soil surface and focus removal of moisture within the rooted part of the soil profile. C_3 and C_4 type plants are adapted to different levels of CO_2, light intensity, and water stress due to variations in metabolic pathways for photosynthetic carbon fixation. C_3 plants are adapted for productivity under moderate soil and air temperatures and light intensities, and are most active during spring and fall in arid environments. However, C_3 plants may be active when water is available during the warmest summer months, in spite of high temperatures, due to stomatal regulation, solar tracking, leaflet closure, low leaf area index, photosynthetic stems, leaf waxes, and varying root profiles that maximize water uptake after precipitation events (Villagra et al., 2011; Giordano et al., 2011; Guevara et al., 2010; Meglioli et al., in press). C_4 plants, including most grasses in arid regions, are generally adapted to high water and temperature stress and low pCO_2, enhancing soil dewatering during summer, so it is expected that carbonate $T(\Delta_{47})$ values will be high in regions of high ratios of C_4 to C_3 plant biomass (Breecker et al., 2009; Meyer et al., 2014). If vegetation type influences site-to-site variability in $T(\Delta_{47})$ records, paleoenvironmental interpretations of formation temperatures may be significantly complicated, as C_4/C_3

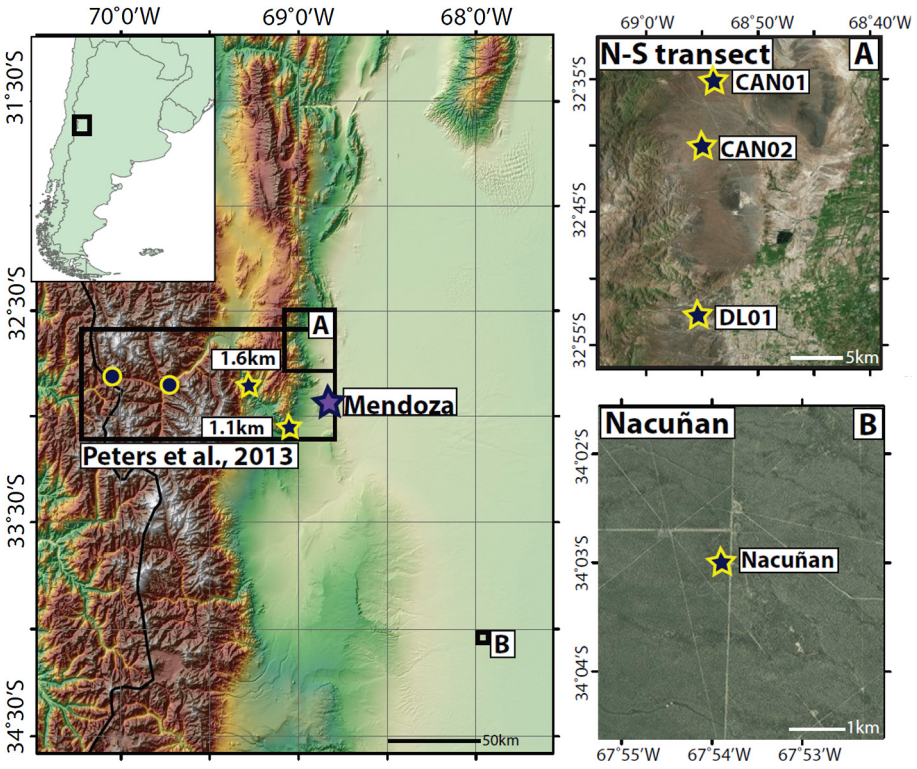

Fig. 1. Eastern Andean piedmont of central Argentina, ~32–34°S. *Left:* Peters et al. (2013) transect with subsurface monitoring sites at 3.2 km, 2.4 km (*circles*, not considered in this study), 1.6 km and 1.1 km (*stars*). *Right:* Inset A: locations (*stars*) of CAN01, CAN02, and DL01 subsurface monitoring sites. Inset B: location of Nacuñan Nature Reserve site.

distribution may be altered by changes in elevation, climate, and land use over time.

2.2. General sampling site description

We sampled pedogenic carbonate from the eastern Andean piedmont of Argentina at 32–34°S in the Villavicencio (CAN01, CAN02), Divisadero Largo (DL01), and Nacuñan Nature Reserves (Fig. 1). The piedmont is an arid, gently eastward sloping topographic feature; the western edge borders the Andes at ~1000 m elevation, sloping down to ~500 m at the eastern edge. The entire piedmont experiences spatially discontinuous summer convective precipitation with infrequent westerly precipitation events rarely reaching its western edge during winter (Mancini et al., 2005). MAAT recorded at Mendoza (~830 m elevation) is ~17 °C and mean annual precipitation (MAP) is ~220 mm (1989–2015) (Base de Datos Hidrológica Integrada (BDHI, http://bdhi.hidricosargentina.gov.ar) and Servicio Meteorológico Nacional (SMN, http://www.smn.gov.ar)). Vegetation type and cover density across the piedmont trend from a nearly 50/50 C_4/C_3 grass mixture at 1000 m elevation in the west to a 90/10 grass mixture at 600 m in the east, with size and density of shrubs and trees increasing to the east (Caravagno, 1988). Soils of the western piedmont are developed in a coarse-grained alluvial conglomerate parent material and contain stage I/II carbonate development (continuous clast undercoatings) (Gile et al., 1966; Birkeland, 1999). Cosmogenic nuclide dating of tectonically uplifted terraces in the otherwise contiguous piedmont between Villavicencio and Mendoza yield ages between 21 and 0.7 ka, highest to lowest, respectively (Schmidt et al., 2011). Our soil pits are adjacent to these terraces but not tectonically disturbed, thus we suggest that surface ages are <5000 yrs.

The Nacuñan Nature Reserve is located ~150 km to the southeast of Mendoza at 34°S. This region also experiences summer-only precipitation, with MAAT ~16 °C and MAP ~326 mm (Ojeda et al., 1998). Plant productivity here is higher than at the Villavicencio and Divisadero Largo sites, although the total C_4/C_3 distribution (grasses and shrubs) is similar to Villavicencio. The soil is modern, based on radiocarbon dating of carbonate nodule samples (Section 3.1), and consists of medium- to coarse-grained sand that contains carbonate nodules.

Extensive prior work in this region (across an E–W transect through the Río Mendoza valley) provides context for our study, including documentation of the elevation dependence of $\delta^{18}O$ values in precipitation, river water, and pedogenic carbonate (e.g. Hoke et al., 2009, 2013), and associated soil carbonate clumped isotope records (e.g. Peters et al., 2013). Data from the 2 nearest Peters et al. (2013) sites are provided for comparison with our results (Figs. 1, 3–4).

3. Methods

3.1. Field station characterization and sampling

In order to investigate the impact of local factors on soil carbonate growth and $T(\Delta_{47})$, we collected modern soil carbonates for $T(\Delta_{47})$ and ^{14}C analysis as well as *in-situ* field data on subsurface conditions (soil temperature, moisture, pCO_2, rooting depth, substrate, carbonate stage), meteorological conditions (air temperature, rainfall, relative humidity, insolation) and vegetation. In July 2013, four soil pits were excavated over a ~40 km N–S transect between the Villavicencio and Divisadero Largo Nature Reserves (~32.7°S) (Fig. 1, Table 1). Two pits (CAN01 and CAN02), separated by ~6 km, were instrumented with Onset soil temperature sensors (10, 50, and 100 cm) and moisture sensors (50 cm) connected to an Onset microstation data logger (Fig. 2a). A pendant temperature logger mounted in a radiation shield was suspended from a pole at 1.5 m above the ground surface. A third pit (DL01) was instrumented with soil temperature and moisture sensors at 10 and 50 cm depth. Stage I–II pedogenic carbonate undercoatings on non-carbonate clasts were collected from these sites at

Table 1
Soil pit and meteorological station locations.

Soil pit site:	Location		Elevation (m)	Data available
	Latitude (S)	Longitude (W)		
CAN01	32°35′31″	68°54′19″	~1000	Soil T (10, 50, 100 cm), Soil Moisture (50 cm), Carbonate undercoatings collected to 1 m depth
CAN02	32°39′07″	68°55′00″	~1000	Soil T (10, 50, 100 cm), Soil Moisture (50 cm) Carbonate undercoatings collected to 1 m depth
CAN03	32°34′12″	68°56′34″	~1000	No instrumental data, Carbonate undercoatings collected at 50 cm depth
DL01	32°52′40″	68°55′21″	~1000	Soil T (10, 50 cm), Soil Moisture (10, 50 cm) Carbonate undercoatings collected to 1 m depth
Nacuñan	34°02′60″	67°54′10″	~540	Soil T (10, 50, 100 cm), Soil Moisture (10, 50, 100 cm), CO_2 (50 cm), Air T, Precip., Insolation, Carbonate nodules collected to 1 m depth
Peters et al. (2013) (1.1 km)	33°02′38″	69°00′33″	~1100	Soil T (10, 50, 100 cm), Soil Moisture (50 cm), Carbonate undercoatings collected to 1 m depth
Peters et al. (2013) (1.6 k)	32°49′24″	69°17′55″	~1600	Soil T (10, 50, 100 cm), Soil Moisture (50 cm), Carbonate undercoatings collected to 1 m depth
Meteorological station:	**Latitude (S)**	**Longitude (W)**	**Elevation**	**Data available**
BDHI: Mendoza	33°00′54″	69°07′03″	~1000	Precip. (1983–2015)
NCDC: Mendoza Airport	32°49′59″	68°46′59″	~1000	Air T, precip. (1959–2015)
NCDC: Mendoza Observatory	32°53′00″	68°51′00″	~1000	Air T, precip. (1959–2015)
GNIP: Mendoza Observatory	32°52′48″	68°51′00″	~1000	Air T, precip., δD, δ^{18}O (1982–1988, 1998–1999)
GNIP: Nacuñan	34°01′48″	67°58′12″	~540	Air T, precip., δD, δ^{18}O (1982–1984)
BDHI: San Rafael	34°36′44″	68°18′58″	~1000	Precip. (1984–2014)

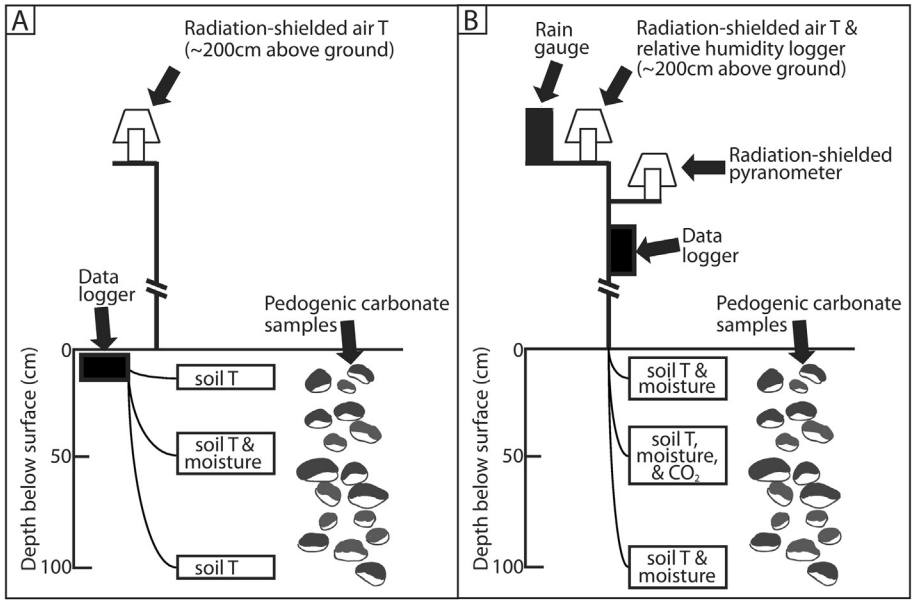

Fig. 2. (**a**) CAN01 and CAN02 site sensor instrumentation (from Peters et al., 2013). (**b**) Nacuñan soil and atmospheric sensor instrumentation.

15–20 cm intervals to 1 m depth. The fourth pit (CAN03) was sampled for carbonate undercoatings at 50 cm depth. The substrate for each soil pit was cobble to boulder conglomerate. A fifth pit was sampled for carbonate nodules to 1 m depth in the Nacuñan Nature Reserve (~34°S; Fig. 1, Table 1). This pit was instrumented with Onset soil moisture and temperature sensors at 10, 50, and 100 cm depth, a Vaisala pCO_2 sensor at 50 cm depth, and Onset air temperature, relative humidity, insolation, and rain sensors (Fig. 2b). Readings from all instruments were logged at 15-minute intervals by an Onset U30-NRC logger (July 2013–May 2015); all sensors were tested prior to deployment in the field for proper functionality, and resulting data were calibrated according to the sensor manufacturer. Vegetation estimates of biomass as % cover were collected using point intercept surveys conducted in representative, undisturbed areas near each soil pit at the end of the *in-situ* monitoring study in April–May 2015.

We complemented our *in-situ* observations with data from nearby weather stations. Daily precipitation data are available from BDHI for Mendoza Airport (near CAN01 and CAN02) and for San Rafael (<100 km southwest of Nacuñan). Daily air temperature and precipitation data are available from NOAA's National Climatic Data Center (NCDC) (http://www.ncdc.noaa.gov/) at Mendoza Airport and Mendoza Observatory. Limited daily air temperature, precipitation, and δD and δ^{18}O data are available from Hoke et al. (2013) and for Mendoza Observatory and Nacuñan through the Global Network of Isotopes in Precipitations (GNIP) (http://www.naweb.iaea.org/napc/ih/IHS_resources_gnip.html).

Table 2
Vegetation description with biomass estimated by % cover.

	CAN01	CAN02	DL01	Nacuñan
% bare soil	25	22	3	0
C_4/C_3 grasses	4.80	36.00	0.10	2.80
C_4/total vegetation cover	0.32	0.46	0.02	0.42
Dominant grasses (C_3 or C_4)	• *Pappophorum* (C_4) • *Bouteloa barbata* (C_4) • *Eragrostis* (C_4)	• *Pappophorum* (C_4) • *Bouteloa barbata* (C_4) • *Eragrostis* (C_4)	• *Jarava ichu* (formerly *Stipa ichu*) (C_3)	• *Pappophorum caespitosum* (C_4) • *Trichloris crinita* (C_4) • *Setaria mendocina* (C_4) • *Jarava ichu* (formerly *Stipa ichu*) (C_3)
Dominant CAM (cacti) (C_4)	• *Opuntia* (C_4) • *Tephrocactus* (C_4)	• *Opuntia* (C_4) • *Tephrocactus* (C_4)		
Dominant shrubs (C_3)	• *Lycium tenuispinosum* • *Larrea cuneifolia* • *Zucagnia punctata*	• *Lycium tenuispinosum* • *Larrea cuneifolia* • *Zucagnia punctata*	• *Trycicla spinosa* • *Lycium tenuispinosum* • *Verbena aspera*	• *Larrea cuneifolia* • *Larrea divaricata* • *Lycium tenuispinosum* • *Prodopsis flexuosa* • *Geoffroea decorticans*

3.2. Stable isotopic analysis and radiocarbon dating methods

Carbonate undercoatings from the piedmont soils were scraped from multiple non-carbonate clasts of the same depth, powdered, and homogenized with an agate mortar and pestle. Carbonate nodules from the sandy soil at Nacuñan were crushed and homogenized, with care taken to remove roots and obvious organic material.

The samples were analyzed at the University of Washington's IsoLab in December 2013 and July 2014. Carbonate samples and standards (8 mg calcite) were digested in 105% phosphoric acid at 90 °C with the evolved CO_2 gas purified using an automated stainless steel vacuum line. The CO_2 was analyzed on a Thermo MAT 253 mass spectrometer configured to measure m/z 44–49 inclusive. Values of $\delta^{13}C$, $\delta^{18}O$, Δ_{47}, and Δ_{48} were calculated using established methods (Eiler and Schauble, 2004; Affek and Eiler, 2006; Huntington et al., 2009 and references therein), with Δ_{47} values corrected to the Absolute Reference Frame (ARF) of Dennis et al. (2011) using heated gas (1000 °C) and CO_2–water equilibration (4 and 60 °C) lines constructed during the analysis period. Samples with Δ_{48} values higher than 2‰, indicating contamination, were rejected. Select samples were also analyzed for $\delta^{13}C$ and $\delta^{18}O$ using a Kiel III carbonate device coupled to a Thermo-Finnigan Delta Plus isotope ratio mass spectrometer (noted in Table 3), following the methods of Tobin et al. (2011).

$T(\Delta_{47})$ values were calculated using the synthetic carbonate calibration of Kluge et al. (2015), which was developed using analytical methods similar to our own (e.g. acid digestion at 90 °C), as well as that of Zaarur et al. (2013) (e.g. acid digestion at 25 °C), for reference. For the range of Δ_{47} values reported in this study (0.572–0.639‰, Table 3), the two calibrations result in similar $T(\Delta_{47})$ estimates, differing by an average of 6% (~2 °C) for samples with $n = 3$ replicates. $T(\Delta_{47})$ values from samples with $n = 3$ replicates are generally recorded to 4–6 °C precision (1 SE).

The Δ_{47} data for soil carbonates from nearby sites by Peters et al. (2013) were reported relative to heated gases only and are not directly comparable to data reported in the ARF. To facilitate direct comparison of the Peters et al. (2013) dataset with the results of this study, splits of their same 50 cm depth samples (1.1 and 1.6 km sites) were reanalyzed at the University of Washington in April 2015.

Radiocarbon dating was performed by DirectAMS (www.directams.com). Pedogenic carbonate samples were digested in phosphoric acid under vacuum to produce CO_2. A disposable manifold was used to transfer the CO_2 to an individual reaction vessel containing zinc and an inner vial of iron dust, which was heated at 550 °C for ~5 h to form graphite. Samples were analyzed on a National Electrostatics Corporation 1.55DH-1 Pelletron Accelerator (0.3% precision and accuracy).

4. Results

4.1. Vegetation survey, radiocarbon ages, and in-situ soil monitoring results

CAN01 and CAN02 lie in a mixed C_4/C_3 vegetation environment dominated by C_3 shrubs with a C_4 grass layer (Table 2). DL01 is dominated by C_3 grasses and shrubs with a higher plant cover than the CAN sites, which may be due to the slight southern aspect of this terrace, which receives lower irradiance than the more exposed CAN sites. Nacuñan lies in a mixed C_4/C_3 environment with the highest productivity of the four sites, including a dominantly C_4 grass layer and a high density of C_3 shrubs.

Radiocarbon dating of pedogenic carbonate undercoatings collected at 40 cm depth at DL01 produced an age of 2080 ± 30 (1σ) yrs BP, and nodules collected at 30, 50, and 100 cm depth at Nacuñan produced ages of 5900 ± 30, 11 140 ± 40, and 16 200 ± 70 yrs BP, respectively, indicating Late Pleistocene to present carbonate formation.

At least 1.5 yrs of data at 15 min intervals are available for each instrumented soil pit, beginning in July 2013. We report air temperature data for CAN01, CAN02, and Nacuñan. Nacuñan soil pCO_2 is available from mid-February 2014 through May 2015; missing data prior to February 2014 was due to a blown fuse in the CO_2 sensor solar power system. Other minor gaps in data collection stem from dead batteries (CAN01), micrologger leaks (CAN01, DL01), and damage from rodent activity (DL01). Daily averaged data sets for all sites are available in the Supplementary Materials.

Total precipitation during our instrument deployment was similar to or greater than historical MAP, whereas average air temperatures reflected historical MAAT. The total precipitation for August 2013–August 2014 for CAN01, CAN02, and DL01 was between 260 (Mendoza Airport) and 280 mm (Mendoza Observatory), exceeding MAP (220 mm) by ~20%. The total precipitation for August 2013–August 2014 recorded by our Nacuñan rain gauge was ~430 mm, exceeding MAP (326 mm) by ~30%. The total precipitation for August 2014–May 2015 was ~160 mm for Mendoza and 280 mm for Nacuñan, falling below the historical average for each site by at least 10%. Average air temperatures at Mendoza and Nacuñan reflected the historical MAAT's of 17 °C and 16 °C, respectively, with daily averaged air temperatures of 0–35 °C. Solar radiation for Nacuñan ranged from 0–1275 W/m^2, with maximum insolation occurring between December and March of each year.

Soil temperatures were comparable for all 4 instrumented pits and similar to those of the two nearest sites (1.1 and 1.6 km) of Peters et al. (2013) (Fig. 3). Average daily soil temperatures ranged from 0–40 °C (10 cm depth) and from 8–35 °C (50 and 100 cm depth) for all 4 sites. Peters et al. (2013) sensor data

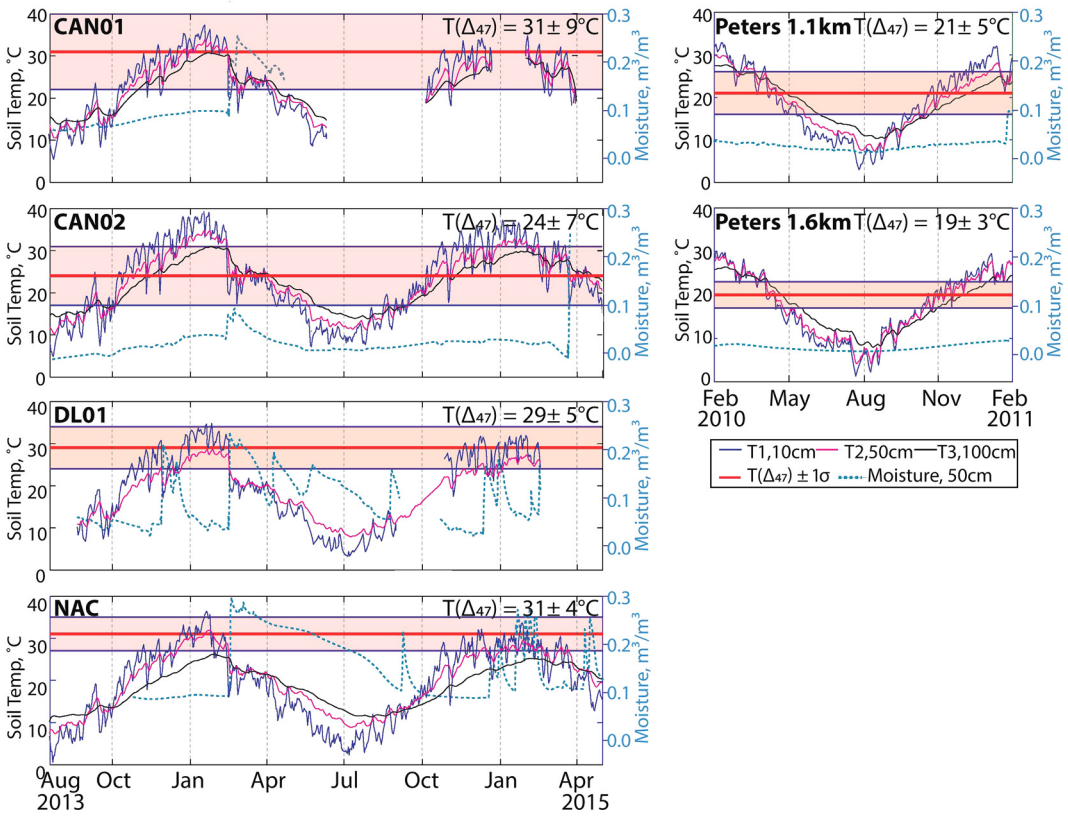

Fig. 3. *In-situ* station records averaged daily for August 2013–May 2015 overlaid with T(Δ_{47}) values (averaged for samples ≥40 cm depth) (*this study*); *in-situ* records for February 2010–January 2011 and T(Δ_{47}) values (Peters et al., 2013).

from 2010 reported soil temperatures of 0–33 °C, air temperatures similar to historical MAAT recorded by nearby weather stations (Guido, 15 °C; Cachueta, 13 °C), and precipitation ~30% below MAP.

We recorded soil wetting and drying events at each instrumented site, observing soil moistures between 0.00 and 0.30 m^3/m^3. According to the sensor manufacturer (Onset), soil moistures of 0.30–0.50 m^3/m^3 represent wet to saturated soils and values <0.10 m^3/m^3 reflect "oven dry" to "dry" soils. A significant wetting event was captured at 50 cm depth for all sites in late February 2014, although conditions at CAN02 during this event remained "dry" (peak soil moisture of 0.09 m^3/m^3). DL01 captured 5 additional soil-wetting events at 50 cm depth, occurring in December 2013, April 2014, and December 2014. Sensors at Nacuñan captured 1 wetting event at 100 cm depth in late February 2014 and a series of wetting events at 50 cm depth in December 2014–April 2015. Soils at all 4 sites typically required less than one month to dry to background moisture conditions after wetting events at 50 cm depth, with the exception of the February 2014 rainstorm, which required 2 (CAN01/CAN02/DL01) to 6 (Nacuñan) months to dry to background conditions.

Soil gas CO_2 rose in response to rainfall during the growing season. Nacuñan soil gas CO_2 recorded at 50 cm depth ranged between 0.12 and 0.60% from February 2014–May 2015, with maximum CO_2 occurring in late February–April 2014. CO_2 concentrations rose sharply in the middle of the growing season after the late February 2014 rainstorm (>170 mm over 3 days resulting in infiltration to 1 m depth (Fig. 5)). Soil CO_2 fell to background levels by late May 2014 and remained low through May 2015, with slight responses to rainfall in summer February–April 2015.

4.2. Isotopic results

Isotopic results are summarized in Table 3 and Fig. 4 (see Supplementary Materials for a full summary of replicate analyses). Soil carbonate $\delta^{13}C$ (range: −6.0 to −0.3‰ (VPDB)) and $\delta^{18}O$ (range: −8.0 to 2.3‰ (VPDB)) generally decrease with depth. Below 50 cm, $\delta^{13}C$ and $\delta^{18}O$ range from −6.0 to −2.1‰ and −8.5 to −0.1‰, respectively. $\delta^{18}O_{SW}$ values (range: −4.9 to 4.9‰ (VSMOW)) were calculated from carbonate $\delta^{18}O$ and T(Δ_{47}) following Kim and O'Neil (1997) and generally decrease with depth for all pits (Table 3). Below 50 cm depth, $\delta^{18}O_{SW}$ values for CAN01, CAN02, and DL01 are similar (range: 0.3 to 2.6‰), while values for Nacuñan are more negative (range: −4.9 to −3.5‰).

Sample Δ_{47} values range from 0.572 to 0.639‰, corresponding to T(Δ_{47}) values of 43 to 20 °C, respectively, using the Kluge et al. (2015) calibration; T(Δ_{47}) values using the Zaarur et al. (2013) calibration lie within 1 standard error of these values (range: 37 to 21 °C). Sample replicate analyses (reported in the ARF following Kluge et al., 2015) of aliquots of the same powders analyzed by Peters et al., 2013 at Caltech (pre-ARF, following Ghosh et al. (2006a)) differ by <2 °C. T(Δ_{47}) values for our study and for Peters et al. (2013) are plotted in Fig. 4.

Average T(Δ_{47}) values are similar for nearby piedmont sites and do not vary systematically with depth. The mean piedmont T(Δ_{47}) is 30 ± 6 °C (±1SE) and Nacuñan T(Δ_{47}) is 29 ± 4 °C; average T(Δ_{47}) values for samples ≥40 cm depth were 28 ± 6 °C and 31 ± 4 °C, respectively. Comparing individual sites, T(Δ_{47}) for CAN01 and CAN02 samples ≥40 cm depth (31 ± 8 °C and 25 ± 7 °C, respectively) are statistically different ($T = 3.13$, $P < 0.05$), though no other pairings between the four sites produced statistically different T(Δ_{47}) values. A one-way ANOVA test indicated that there were no statistical differences between the four groups using a significance threshold of 0.05 (95%; see Supplementary Materials).

Table 3
Summary of carbonate sample isotopic analyses.

Sample:	*n*	$\delta^{13}C$[a] (‰) (VPDB)	$\delta^{18}O$[a] (‰) (VPDB)	$\Delta_{47} \pm 1SE$[a] (‰)	$T(\Delta_{47}) \pm 1SE$ (°C)		Soil water $\delta^{18}O$[b] (‰) (VSMOW)	
				Calibration:	Kluge et al. (2015)	Zaarur et al. (2013)	Kluge et al. (2015)	Zaarur et al. (2013)
CAN01, 1.0 km elevation								
10 cm	3	−1.8	−3.7	0.572 ± 0.011[c]	43 ± 4	37 ± 3	2.1 ± 0.9	1.0 ± 0.6
25 cm	3	−0.3	−2.2	0.609 ± 0.012[c]	29 ± 4	28 ± 3	1.0 ± 0.9	0.7 ± 0.7
40 cm	3	−1.9	−3.4	0.601 ± 0.014	32 ± 5	30 ± 4	0.4 ± 1.0	−0.1 ± 0.7
55 cm	3	−3.1	−3.4	0.609 ± 0.013	30 ± 5	28 ± 3	−0.1 ± 0.9	−0.5 ± 0.6
70 cm	2	−3.5	−1.9	0.595 ± 0.018	35 ± 7	31 ± 5	2.4 ± 1.3	1.8 ± 1.0
100 cm	2	−2.6	−3.2	0.612 ± 0.045	29 ± 17	27 ± 11	−0.1 ± 4.6	−0.4 ± 3.5
Avg. ≥40 cm depth:		***−2.8***	***−3.0***	***0.604 ± 0.023***	***31 ± 8***	***29 ± 6***	***1.0 ± 2.0***	***0.2 ± 1.5***
CAN02, 1.0 km elevation								
10 cm	3[d]	−0.9	0.9	0.610 ± 0.011[c]	29 ± 4	28 ± 3	4.2 ± 0.7	3.9 ± 0.5
25 cm	3[d]	−3.1	2.3	0.627 ± 0.011	24 ± 4	23 ± 3	4.4 ± 0.7	4.4 ± 0.5
40 cm	2[d]	−3.7	0.8	0.615 ± 0.013[c]	28± 5	26 ± 3	3.7 ± 0.9	3.5 ± 0.6
55 cm	2[d]	−4.7	−0.1	0.617 ± 0.027	27 ± 9	26 ± 6	2.6 ± 1.8	2.4 ± 1.2
70 cm	3[d]	−2.1	−0.8	0.625 ± 0.017	24 ± 6	24 ± 4	1.4 ± 1.1	1.4 ± 0.8
85 cm	3[d]	−3.9	−1.9	0.639 ± 0.015	20 ± 5	21 ± 3	−0.6 ± 1.0	−0.4 ± 0.7
100 cm	2[d]	−5.0	−1.8	0.615 ± 0.027	28 ± 10	26 ± 7	1.1 ± 1.9	0.9 ± 1.3
Avg. ≥40 cm depth:		***−3.9***	***−0.8***	***0.627 ± 0.020***	***25 ± 7***	***25 ± 5***	***1.7 ± 1.3***	***1.5 ± 0.9***
CAN03, 1.0 km elevation								
50 cm	3	−4.7	−2.9	0.609 ± 0.011[c]	30 ± 4	28 ± 3	0.4 ± 0.8	0.0 ± 0.6
DL01, 1.0 km elevation								
20 cm	3	−1.2	−1.0	0.584 ± 0.011[c]	39 ± 4	34 ± 3	4.0 ± 0.8	3.2 ± 0.5
40 cm	4	−4.1	−1.4	0.630 ± 0.019	23 ± 6	23 ± 5	0.5 ± 1.3	0.6 ± 0.9
70 cm	2	−5.2	−2.5	0.616 ± 0.013[c]	27 ± 5	26 ± 3	0.3 ± 0.9	0.0 ± 0.7
100 cm	2	−5.2	−3.0	0.590 ± 0.013[c]	36 ± 5	32 ± 3	1.6 ± 1.4	1.9 ± 1.1
Avg. ≥40 cm depth:		***−4.8***	***−2.3***	***0.612 ± 0.015***	***29 ± 5***	***27 ± 4***	***0.8 ± 1.2***	***0.5 ± 0.8***
Nacuñan, 0.6 km elevation *(carbonate nodule samples)								
20 cm	3	−5.5	−6.7	0.634 ± 0.012	21 ± 4	22 ± 3	−5.1 ± 0.9	−5.0 ± 0.7
50 cm	4[d]	−6.0	−8.3	0.585 ± 0.011	38 ± 4	34 ± 3	−3.4 ± 0.8	−4.2 ± 0.6
85 cm	3[d]	−5.7	−7.6	0.622 ± 0.011[c]	25 ± 4	25 ± 3	−5.2 ± 0.7	−5.3 ± 0.5
100 cm	2	−5.5	−8.5	0.605 ± 0.013[c]	31 ± 5	29 ± 3	−5.0 ± 1.2	−5.4 ± 0.9
Avg. ≥40 cm depth:		***−5.7***	***−8.1***	***0.604 ± 0.012***	***31 ± 4***	***29 ± 3***	***−4.5 ± 0.9***	***−5.0 ± 0.7***
Peters et al. (2013), 1.1 km elevation								
50 cm, 2013		−5.9	−1.2	0.686 ± 0.019	*Pre-ARF:*	17 ± 4	*Pre-ARF:*	−0.5 ± 0.9
50 cm, 2015		−5.9	−1.7	0.645 ± 0.019	*ARF, Kluge:*	18 ± 4	*ARF, Kluge:*	−0.8 ± 0.9
Pit average:		***−5.1***[e]	***−2.7***[e]	***0.671 ± 0.023***[c]	***Pre-ARF:***	***20 ± 4***	***Pre-ARF:***	***−1.4 ± 0.7***
Peters et al. (2013), 1.6 km elevation								
50 cm, 2013		−5.5	−9.7	0.688 ± 0.019	*Pre-ARF:*	16 ± 3	*Pre-ARF:*	−9.2 ± 0.6
50 cm, 2015		−5.9	−9.6	0.663 ± 0.019	*ARF, Kluge:*	13 ± 3	*ARF, Kluge:*	−9.9 ± 0.7
Pit average:		***−6.0***[e]	***−10.5***[e]	***0.675 ± 0.013***[e]	***Pre-ARF:***	***19 ± 3***	***Pre-ARF:***	***−9.4 ± 0.6***

[a] Carbonate $\delta^{13}C$, $\delta^{18}O$, reported as mean and Δ_{47} reported as weighted mean of replicates (*n*) for each individual sample. Average external error (1SE) for replicates of a sample is ±0.03‰ for $\delta^{13}C$ and for $\delta^{18}O$, and ±0.019‰ for Δ_{47}.

[b] Soil water $\delta^{18}O$ was calculated using the calcite–water O-isotope fractionation equation of Kim and O'Neil (1997). Uncertainty in soil water $\delta^{18}O$ was calculated by propagating errors in $T(\Delta_{47})$.

[c] For samples with low SE for replicates, SE was assigned using the long-term SD of a standard run during the same period of time divided by sqrt(*n*), where *n* is the number of sample replicates, following Peters et al. (2013) and Huntington et al. (2009).

[d] Samples noted with n^d were analyzed using an additional two replicates for $\delta^{13}C$ and $\delta^{18}O$ measurements using a Kiel III Carbonate Device coupled to a dual-inlet Thermo Finnigan Delta Plus IRMS at the University of Washington Isolab.

[e] Peters et al. (2013) (pre-ARF) average external error (1SE) for replicates is ±0.04‰ for $\delta^{13}C$, ±0.002‰ for $\delta^{18}O$, and ±0.016‰ for Δ_{47}.

The $T(\Delta_{47})$ of the single sample at the fifth site (30 ± 4 °C, 50 cm depth) did not differ from the mean values of the other sites.

$T(\Delta_{47})$ values for all 4 instrumented pits are comparable to recorded summer soil temperatures (Fig. 3). For CAN01, DL01, and Nacuñan, $T(\Delta_{47})$ values are similar to soil temperatures only during the hottest summer months, while CAN02 values reflect late spring and late summer soil temperatures. $T(\Delta_{47})$ values exceed MAAT and MAST and equal or exceed the average hottest monthly mean soil temperature (HMST) at 50 cm, with the exception of CAN02, which falls between MAST and HMST (Fig. 4). The $T(\Delta_{47})$ values of Peters et al. (2013) (1.1 km and 1.6 km sites) more closely approach local MAST and are similar to soil temperatures in late spring, early fall, and for a brief period during summer (January 2011); these values exceed MAAT and fall between MAST and HMST.

5. Discussion

5.1. Radiocarbon ages and C and O isotope trends

Radiocarbon analyses for carbonate coatings at DL01 and nodules at Nacuñan produced ages ≤16 ky, consistent with the early stage (Gile et al., 1966) and small nodule size (Retallack, 2005) of Holocene/Late Pleistocene pedogenic carbonates. ^{14}C is incorporated into coatings or nodules as soil carbonates grow over time, resulting in time-averaged radiocarbon ages that are typically interpreted as underestimates of the true age of carbonate formation (Amundson et al., 1993; Yang et al., 1994). However, the difference

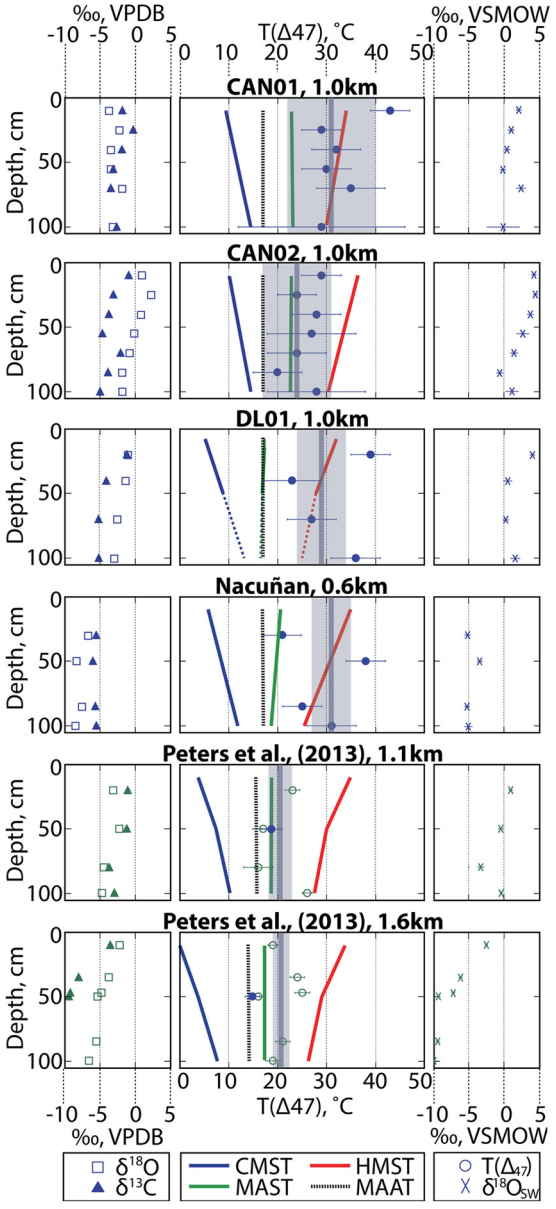

Fig. 4. Soil carbonate isotope data from this study (blue symbols) and from Peters et al. (2013, green symbols). *Left panels:* carbonate $\delta^{13}C$ (VPDB, triangles) and $\delta^{18}O$ (VPDB, squares) values. *Middle panels:* soil carbonate $T(\Delta_{47}) \pm 1SE$ calculated using equation (5) of Kluge et al. (2015) (*blue circles:* this study; *green circles:* Peters et al., 2013). Gray vertical bars and shaded boxes indicate the mean and standard deviation across $T(\Delta_{47})$ for samples $\geq$40 cm depth in a soil profile. Lines represent coldest mean soil temperature (CMST, blue), mean annual soil temperature (MAST, green), hottest mean soil temperature (HMST, red), and mean annual air temperature (MAAT, black), extrapolated from 1.5 yrs of soil temperatures recorded at 10, 50, and 100 cm depth, and from air temperatures recorded at Mendoza Airport (CAN01, CAN02, DL01) and by instrumentation at Nacuñan. *Right panels:* calculated $\delta^{18}O_{SW}$ (VSMOW, crosses). (For interpretation of the references to color in this figure legend, the reader is referred to the web version of this article.)

between true age and radiocarbon age is likely greater at the surface than at depth because near-surface soil carbonate may more easily be contaminated with younger ^{14}C. Indeed, at Nacuñan ages increase systematically with depth from ~6 to 16 ky BP, matching theoretical predictions (Yang et al., 1994). The frequency of carbonate-forming events may also impact radiocarbon ages: if carbonates form more frequently at the surface than at depth due to frequent shallow soil wetting events, the incorporation of additional, younger ^{14}C may produce more recent radiocarbon ages nearer the surface. Overall, radiocarbon analyses for nodules at Nacuñan suggest Holocene/Late Pleistocene formation in relatively stable soil.

Carbonate $\delta^{13}C$ and $\delta^{18}O$ values generally increase towards the surface, indicating undisturbed soil profiles with near-surface soil water evaporation and soil gas exchange with atmospheric CO_2. Below 50 cm depth, the range of $\delta^{13}C$ values reflects mixed C_4/C_3 environments with lower soil productivity at CAN01 and CAN02 (−5.0 to −2.1‰) than at DL01 and Nacuñan (−6.0 to −5.2‰), which is supported by our vegetation coverage survey (Table 2; Cerling and Quade, 1993).

5.2. Potential for site-to-site variability in $T(\Delta_{47})$

Despite potential differences in soil productivity and C_4/C_3 distribution, $T(\Delta_{47})$ values averaged over depth for our soil profiles are not significantly different. This suggests that nearby sites in a single precipitation regime at a single elevation will be indistinguishable in $T(\Delta_{47})$ even under varying C_4/C_3 distributions within the 4–6 °C resolution ($n = 3$ replicates) of the clumped isotope method. This challenges the expectation that soil carbonate formation temperatures will be higher under C_4 than under C_3 plant growth (e.g. Breecker et al., 2009; Meyer et al., 2014), and agrees with phenological and ecophysiological studies that show C_3 plant activity during wet pulses, in spite of warm temperatures (Meglioli et al., in press; Villagra et al., 2011; Giordano et al., 2011). Additionally, no difference was found between sites with carbonate undercoatings (piedmont sites) and nodules (Nacuñan).

However, while $T(\Delta_{47})$ values are indistinguishable among our sites, our values exceed those of the nearest two sites studied by Peters et al. (2013) by ~10 °C, despite comparable surface and *in-situ* temperature conditions. Peters et al. (2013) suggested that the average ~20 °C $T(\Delta_{47})$ value for their sites was due to the summer-focused rainfall in this region, which could result in soil drying and carbonate formation during late fall when soils are closer to MAST than HMST. According to our sensor data, while soils may be wet from mid-summer through fall, carbonate formation in response to the early stage of soil drying or between discrete summer rain events could significantly impact $T(\Delta_{47})$, resulting in hot summer values. The ~10 °C difference between these two studies suggests that there is a potential for substantial spatial variability in $T(\Delta_{47})$ at the same elevation in a region dominated by the same precipitation and vegetation regime. The nearest Peters site (1.1 km) differs from DL01 by only 100 m elevation and 20 km distance; it may be possible that local hydrology, topographic features, or differences in soil water chemistry may contribute to a difference in the timing and temperature of carbonate formation. In particular, the Peters 1.1 km site lies <0.5 km from the Mendoza River, which transports limestone rich sediment from the high Andes and causes periodic flooding that could alter soil moisture and chemistry in this site. Flooding and subsequent soil drying in winter, spring, or fall could have contributed to decreased $T(\Delta_{47})$ values, although further investigation into the age, frequency of flooding, and sub-surface physical and chemical characteristics of these sites would be necessary to say more about potential impacts on carbonate formation. The location of the Peters 1.6 km site in a narrow, N–S portion of the Río Mendoza valley may also influence local productivity and soil hydrology, which could contribute to the difference in $T(\Delta_{47})$ values between these studies.

5.3. Invariance of $T(\Delta_{47})$ with depth

$T(\Delta_{47})$ values from each sampled pit did not vary systematically or decrease towards MAST with depth (Fig. 4), consistent with data from other studies (Quade et al., 2013; Peters et al., 2013).

The simplest explanation for this invariance would be carbonate formation during spring or fall when the soil profile is near isothermal, such that the range of $T(\Delta_{47})$ values would be constrained through the soil profile. Our instrumental records show that the conditions for a seasonally isothermal soil occur over a narrow range of time (1–2 weeks) during the spring and fall in which soil temperatures are near MAAT. However, our observed $T(\Delta_{47})$ values range from 24–31 °C, at least 6–10 °C higher than MAAT, spring, or fall soil temperatures at any instrumented pit. This discrepancy is more than can be explained by temperature fluctuations that may have occurred over the hundreds to thousands of years required for soil carbonate formation processes to occur in these sites, suggesting that some other process must account for the observed temperature invariance with depth.

5.4. Isothermal conditions after rainfall events

Generally, *in-situ* soil temperatures recorded at all four sites immediately following significant soil wetting events are similar to carbonate formation $T(\Delta_{47})$ values and reflect the isothermal conditions seen in our $T(\Delta_{47})$ profiles. High frequency variations in near-surface temperature and moisture may explain some of the scatter in $T(\Delta_{47})$ values with depth. However, since $T(\Delta_{47})$ is generally consistent with depth, averaging values throughout a soil profile should provide a robust measure of average soil temperatures following rainfall events. Soil moisture sensors at all sites captured soil wetting at 50 cm depth after a large late February 2014 rainstorm, immediately after which near-isothermal conditions were registered at 10, 50, and 100 cm (Fig. 3). In the first 1–3 days following this event, soil temperatures at CAN01 converged at ~30 °C, within the range of uncertainty of $T(\Delta_{47})$ for this site (Fig. 3). During the months after this event when the soil was drying back to baseline conditions, soil temperatures fell well below the range of $T(\Delta_{47})$ values for this site, such that carbonate formation later in the drying curve would result in lower $T(\Delta_{47})$ values than we observed at all depths. This infiltration-driven cooling of soil temperatures to isothermal $T(\Delta_{47})$ values in the early part of the soil drying curve is seen after large precipitation events at all sites. If carbonate were to form at these times at any depth in the soil, it would contribute to a warm-season biased, isothermal $T(\Delta_{47})$ depth profile, such as we see in Fig. 4.

If isothermal profiles are not caused by carbonate formation while the soil profile is isothermal, the timing and depth of infiltration may govern formation temperatures at different depths in such a way that hot isothermal $T(\Delta_{47})$'s are reached. At Nacuñan, more than 50% of wetting events recorded at 10 cm depth did not reach the 50 cm soil moisture sensor, and 90% of wetting events recorded at 50 cm depth did not reach the 100 cm soil moisture sensor. Brief periods of soil drying after small rainstorms with shallow infiltration could result in more frequent carbonate formation near the surface than at depth. These small events occur at Nacuñan throughout the spring, summer, and fall. While spring and fall events could contribute to cooler carbonate formation temperatures, the bulk of precipitation in this region occurs in summer and frequent wetting and drying events during the hottest months could bias $T(\Delta_{47})$ values to seasonal summer soil temperatures. Below 50 cm depth, soil wetting and drying appear to be caused only by large, infrequent mid-summer rainstorms. Hot $T(\Delta_{47})$ values at depth could represent soil carbonate formation during the early part of soil drying immediately after these individual wetting events.

Our findings are consistent with a recent study of soil carbonates from Wyoming and Nebraska by Hough et al. (2013), who used air temperature and soil carbonate $T(\Delta_{47})$ data from a single depth per site to propose that soil carbonate forms during soil drying in early summer and after mid-late summer precipitation. By providing soil temperature, soil moisture, and $T(\Delta_{47})$ data with depth, we build on this work to suggest that high temperatures and isothermal conditions recorded in Δ_{47} signals are accounted for by carbonate formation occurring immediately after precipitation events, and not during the progressive drying out of the soil at the tail end of the wet season, as suggested by Breecker et al. (2009) and Peters et al. (2013), when observed soil temperatures are too low to be reconciled with $T(\Delta_{47})$ values. Furthermore, we suggest that shallow carbonate formation ($\leq$50 cm depth) occurs in response to more frequent precipitation events than carbonate formation deeper in the soil profile. Carbonate $T(\Delta_{47})$ values $\geq$50 cm depth may reflect soil conditions just after large, discrete mid-summer rainstorms, while shallow carbonates integrate $T(\Delta_{47})$ values from formation throughout spring, summer, and fall, with summer soil wetting and drying events dominating the Δ_{47} signal. Under these conditions, carbonates throughout the soil profile could reflect near-isothermal summer formation temperatures, as observed in Fig. 4.

5.5. Conditions of calcite supersaturation

In the context of soil wetting events discussed above, if the soil profile is permanently supersaturated in calcite, it is reasonable to assume that carbonate formation can begin early in the soil drying curve, allowing for the hot, isothermal temperatures occurring immediately after precipitation events at these sites to be recorded in $T(\Delta_{47})$ formation temperature estimates. Permanent calcite supersaturation has been demonstrated in other arid and hyperarid environments (Inskeep and Bloom, 1986; Hamdi-Aissa et al., 2004; Marion et al., 2008). At Nacuñan, significant dust influxes carried by zonda winds from the eastern slope of the Andes contribute to near-saturated Ca^{2+} concentration in surface soils, which should be relatively constant with depth (Jobbagy and Jackson, 2001). As a first-pass estimate for determining the seasonality of $CaCO_3$ supersaturation at Nacuñan, equation (2) was solved using soil temperature and pCO_2 data from 50 cm with the minimum value of Ca^{2+} concentration reported from surface soils (0–20 cm depth) in previous studies at Nacuñan (1.5–2.0 mmol/L; Rossi and Villagra, 2003; Rossi, 2004). Alphas were calculated for February 2014–May 2015, assuming a constant Ca^{2+} concentration of 1.5 mmol/L throughout the year. Estimated $\alpha_{calcite}$ values were always greater than 1, suggesting that persistent conditions of $CaCO_3$ supersaturation should allow for calcite precipitation at any time that water is removed from the soil (Fig. 5). The lowest alpha values occurred in early March 2014, coincident with maximum observed soil pCO_2, and increasing calcite supersaturation was seen as the soil dried out and plant activity declined in winter. While the assumption of constant Ca^{2+} concentration is a considerable oversimplification during soil wetting and soil dewatering by evaporation and root uptake, Ca^{2+} concentration must fall significantly below the measured range (20–50%) under the high soil temperatures and low pCO_2 conditions observed in order to allow for significant calcite dissolution. While it appears that Nacuñan experiences permanent calcite supersaturation that would allow for carbonate formation to begin early in the soil drying curve, resulting in the hot, isothermal $T(\Delta_{47})$ values observed at this site, further information on the distribution of soluble chemical species in this location would be necessary to more accurately demonstrate conditions of permanent or seasonal supersaturation and to predict conditions favoring calcite dissolution or precipitation.

5.6. Implications for isotopic records from pedogenic carbonates

This study results in two key findings that should inform future application of the clumped isotope geothermometer to estimate formation temperatures of pedogenic carbonates.

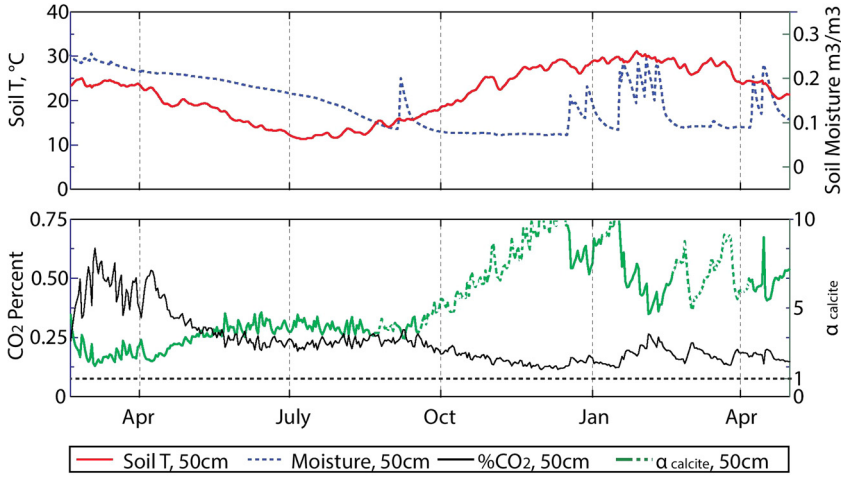

Fig. 5. *In-situ* Nacuñan records (soil temperature, soil moisture, and soil gas CO_2 concentration at 50 cm) with calculated $\alpha_{calcite}$ values, mid-February 2014–May 2015, assuming a constant Ca^{2+} concentration of 1.5 mmol/L. In order for $\alpha_{calcite}$ to fall <1 (favoring calcite dissolution), Ca^{2+} concentration must be reduced by 20% (to 1.2 mmol/L) in March–May 2014 when pCO_2 is highest, by 33% (to <1.0 mmol/L) in May–September 2014, and by 50% (to <0.75 mmol/L) after September 2014. Solid portions of the $\alpha_{calcite}$ line correspond to periods when the soil moisture at 50 cm is >0.1 m^3/m^3.

1) For our four arid sites under the same precipitation regime at similar elevations with varying C_4/C_3 biomass, site-to-site variability in soil carbonate undercoating or nodule $T(\Delta_{47})$ records is negligible, such that $T(\Delta_{47})$ records need not be adjusted to account for vegetation type. However, there is significant variation between $T(\Delta_{47})$ values calculated for this study and for nearby sites in the Río Mendoza valley studied by Peters et al. (2013); we hypothesize that these differences are due to topographic setting and proximity to the Río Mendoza. This suggests the potential for strong local controls on soil hydrology that may result in systematic spatial variations in $T(\Delta_{47})$.

2) $T(\Delta_{47})$ values were found to be invariant to 1 m depth. This suggests that for a summer precipitation regime in a semi-arid region, soil carbonate formation is restricted to intervals when the soil profile is isothermal (occurring during either the transition in seasons or after large soil wetting events), or that a variation in the frequency of soil carbonate formation events at different depths results in hot, isothermal $T(\Delta_{47})$ values. Thus, potential (paleo)precipitation regimes should be carefully considered using soil geochemistry or physical properties (e.g., Retallack, 1994, 2005; Royer, 1999; Hyland and Sheldon, 2013; Hyland et al., 2015) when applying the carbonate clumped isotope geothermometer to paleoenvironmental reconstructions.

6. Conclusions

With its summer-only precipitation regime and C_4/C_3 transition, the eastern Andean Piedmont is an ideal location for investigating the potential influence of vegetation type and site-specific controls on variability in pedogenic carbonate clumped isotope records. While it appears that climatic conditions and C_4/C_3 distributions have varied significantly over the 1000's of years integrated by soil carbonates relative to our <2 yrs of *in-situ* soil and atmospheric data, future work should consider whether the impact of these climate changes can be resolved within the 4–6 °C uncertainty of the clumped isotope record (Gil et al., 2014; Labraga and Villalba, 2008; Silva et al., 2011). We find that carbonate clumped isotope formation temperatures are invariant between sites of ~0.02–0.46 C_4/total vegetation biomass by groundcover, fall at or above HMST, and are near-isothermal between 10 and 100 cm depth. We suggest that isothermal $T(\Delta_{47})$ behavior is due to shallow (≤40 cm) carbonate formation driven by seasonal precipitation biased to frequent summer rainfall, while deeper (≥40 cm) carbonates reflect formation after large, infrequent, and discrete mid-summer rainstorms.

Acknowledgements

We thank Almendra Brasca and Villavicencio, Divisadero Largo, and Nacuñan Nature Reserve park rangers for generous field assistance, and Andy Schauer and Kyle Samek for lab assistance at the University of Washington Isolab. This work was funded by a National Science Foundation grant 1251966 awarded to GDH, and grants 1252064 and 1156134 awarded to KWH. We thank our reviewers and editor for their constructive reviews.

Appendix A. Supplementary material

Supplementary material related to this article can be found online at http://dx.doi.org/10.1016/j.epsl.2016.02.003.

References

Affek, H.P., Eiler, J.M., 2006. Abundance of mass 47 CO_2 in urban air, car exhaust, and human breath. Geochim. Cosmochim. Acta 70, 1–12.

Amundson, R., Wang, Y., Chadwick, O., Trumbore, S., McFadden, L., McDonald, E., Wells, S., DeNiro, M., 1993. Factors and processes governing the ^{14}C content of carbonate in desert soils. Earth Planet. Sci. Lett. 125, 385–405.

Birkeland, P.W., 1999. Soils and Geomorphology. Oxford University Press, New York. 430 p.

Breecker, D.O., Sharp, Z.D., McFadden, L.D., 2009. Seasonal bias in the formation and stable isotopic composition of pedogenic carbonate in modern soils from central New Mexico, USA. Geol. Soc. Am. Bull. 121 (3–4), 630–640.

Caravagno, J.N., 1988. Distribution of C_3 and C_4 grasses at different altitudes in a temperate arid region of Argentina. Oecologia 76, 273–277.

Cerling, T.E., Quade, J., 1993. Stable carbon and oxygen isotopes in soil carbonates. In: Swart, P.K., Lohmann, K.C., McKenzie, J., Savin, S.M. (Eds.), Climate Change in Continental Isotopic Records, Geophysical Monograph. American Geophysical Union, Washington, DC, pp. 217–231.

Dennis, K.J., Affek, H.P., Passey, B.H., Schrag, D.P., Eiler, J.M., 2011. Defining an absolute reference frame for 'clumped' isotope studies of CO_2. Geochim. Cosmochim. Acta 75, 7117–7131.

Drever, J.I., 1982. The Geochemistry of Natural Waters. Prentice Hall, New York. 436 p.

Eiler, J.M., 2007. "Clumped-isotope" geochemistry – the study of naturally-occurring, multiply substituted isotopologues. Earth Planet. Sci. Lett. 262, 209–327.

Eiler, J.M., Schauble, E., 2004. $^{18}O^{13}C^{16}O$ in Earth's atmosphere. Geochim. Cosmochim. Acta 68, 4767–4777.

Gabitov, R.I., Watson, E.B., Sadekov, A., 2012. Oxygen isotope fractionation between calcite and fluid as a function of growth rate and temperature: an in situ study. Chem. Geol. 306–307, 92–102.

Ghosh, P., Adkins, J., Affek, H., Balta, B., Guo, Wl., Schauble, E.A., Schrag, D., Eiler, J.M., 2006a. ^{13}C–^{18}O bonds in carbonate minerals: a new kind of paleothermometer. Geochim. Cosmochim. Acta 70, 1430–1456.
Ghosh, P., Garzione, C.N., Eiler, J.M., 2006b. Rapid uplift of the Altiplano revealed through ^{13}C–^{18}O bonds in paleosol carbonates. Science 311, 511–515.
Gil, A.F., Villalba, R., Ugan, A., Cortegoso, V., Neme, G., Michieli, C.T., Novellino, P., Durán, V., 2014. Isotopic evidence on human bone for declining maize consumption during the little ice age in central western Argentina. J. Archaeol. Sci. 49, 213–227.
Gile, L.H., Peterson, F.F., Grossman, R.B., 1966. Morphological and genetic sequences of carbonate accumulation in desert soils. Soil Sci. 101 (5), 347–360.
Giordano, C., Guevara, A., Boccalandro, H., Sartor, C., Villagra, P.E., 2011. Water status, drought responses, and growth of P. flexuosa trees with different access to the water table in a warm South American desert. Plant Ecol. 212, 1123–1134.
Guevara, A., Giodano, C.V., Aranibar, J.N., Quiroga, M., Villagra, P.E., 2010. Phenotypic plasticity of the coarse root system of Prosopsis flexuosa, a phreatophyte tree, in the Monte Desert (Argentina). Plant Soil 330, 447–464.
Guo, W., 2008. Carbonate clumped isotope thermometry: application to carbonaceous chondrites and effects of kinetic isotope fractionation. Dissertation. California Institute of Technology.
Hamdi-Aissa, B., Valles, V., Aventurier, A., Ribolzi, O., 2004. Soils and brine geochemistry and mineralogy of hyperarid desert playa, Ouargla Basin, Algerian Sahara. Arid Land Res. Manag. 18, 103–126.
Hoke, G.D., Aranibar, J.N., Viale, M., Araneo, D.C., Llano, C., 2013. Seasonal moisture sources and the isotopic composition of precipitation, rivers, and carbonates across the Andes at 32.5–35.5°S. Geochem. Geophys. Geosyst. 14, 962–978.
Hoke, G.D., Garzione, C.N., Araneo, D.C., Latorre, C., Strecker, M.R., Williams, K.J., 2009. The stable isotope altimeter: do quaternary pedogenic carbonates predict modern elevations? Geology 37, 1015–1018.
Hough, C.G., Fan, M., Passey, B.H., 2013. Calibration of the clumped isotope geothermometer in soil carbonate in Wyoming and Nebraska, USA: implications for paleoelevation and paleoclimate reconstruction. Earth Planet. Sci. Lett. 391, 110–120.
Huntington, K.W., Eiler, J.M., Affek, H.P., Guo, W., Bonifacie, M., Yeung, L.Y., Thiagarajan, N., Passey, B., Tripati, A., Daeron, M., Came, R., 2009. Methods and limitation of 'clumped' CO_2 isotope (D47) analysis by gas-source isotope ratio mass spectrometry. J. Mass Spectrom. 44, 1318–1329.
Huxman, T.E., Snyder, K.A., Tissue, D., Leffler, A.J., Ogle, K., Pockman, W.T., Sandquist, D.R., Potts, D.L., Schwinning, S., 2004. Precipitation pulses and carbon fluxes in semiarid and arid ecosystems. Oecologia 141, 254–268.
Hyland, E.G., Sheldon, N.D., 2013. Coupled CO_2-climate response during the Early Eocene Climatic Optimum. Palaeogeogr. Palaeoclimatol. Palaeoecol. 369, 125–135.
Hyland, E.G., Sheldon, N.D., Van der Voo, R., Badgley, C., Abrajevitch, A., 2015. A new paleoprecipitation proxy based on soil magnetic properties: implications for expanding paleoclimatology reconstructions. Geol. Soc. Am. Bull. http://dx.doi.org/10.1130/B31207.1.
Inskeep, W.P., Bloom, P.R., 1986. Calcium carbonate supersaturation in soil solutions of Calciaquolls. Soil Sci. Am. J. 50, 1431–1437.
Jobbagy, E.G., Jackson, R.B., 2001. The distribution of soil nutrients with depth: global patterns and the imprint of plants. Biogeochemistry 53, 51–77.
Kim, S., O'Neil, J.R., 1997. Equilibrium and nonequilibrium oxygen isotope effects in synthetic carbonates. Geochim. Cosmochim. Acta 61, 3461–3475.
Kluge, T., John, C.M., Jourdan, A., Davis, S., Crawshaw, J., 2015. Laboratory calibration of the calcium carbonate clumped isotope thermometer in the 25–250°C temperature range. Geochim. Cosmochim. Acta 157, 213–227.
Labraga, J.C., Villalba, R., 2008. Climate in the Monte Desert: past trends, present conditions, and future projections. J. Arid Environ. 73, 154–163.
Liu, X.Z., Wan, S.Q., Su, B., Hui, D.F., Luo, Y.Q., 2002. Response of soil CO_2 efflux to water manipulation in a tallgrass prairie ecosystem. Plant Soil 240, 213–223.
Luo, Y., Zhou, X., 2006. Soil Respiration and the Environment. Academic Press, Burlington.
Machette, M.N., 1985. Calcic soils of the southwestern United States. Spec. Pap., Geol. Soc. Am. 203, 1–22.
Mancini, M., Paez, M., Prieto, A., Stutz, S., Tonello, M., Vilanova, I., 2005. Mid-Holocene climatic variability reconstruction from pollen recods (32°–52°S Argentina). Quat. Int. 132, 47–59.
Marion, G.M., Verburg, P.S.J., Stevenson, B., Arnone, J.A., 2008. Soluble element distributions in a Mojave desert soil. Soil Sci. Soc. Am. J. 72, 1–9.
Meglioli, P.A., Villagra, P.E., Aranibar, J.N., in press. Does land use change alter water and nutrient dynamics of phreatophytic trees in the Central Monte desert? Ecohydrology. http://dx.doi.org/10.1002/eco.1670.
Meyer, N.A., Breecker, D.O., Young, M.H., Litvak, M.E., 2014. Simulating the effect of vegetation in formation of pedogenic carbonate. Pedol., Soil Sci. Soc. Am. J. 78, 914–924.
Ojeda, R.A., Campos, C.M., Gonnet, J.M., Borghi, C.E., Roig, V.G., 1998. The MaB Reserve of Ñacuñán, Argentina: its role in understanding the Monte Desert biome. J. Arid Environ. 39, 299–313.
Passey, B.H., Levin, N.E., Cerling, T.E., Brown, F.H., Eiler, J.M., Turekian, K.K., 2010. High-temperature environments of human evolution in East Africa based on bond ordering in paleosol carbonates. Proc. Natl. Acad. Sci. USA 107, 11245–11249.
Peters, N.A., Huntington, K.W., Hoke, G.D., 2013. Hot or not? Impact of seasonally variable soil carbonate formation on paleotemperature and O-isotope records from clumped isotope thermometry. Earth Planet. Sci. Lett. 361, 208–218. http://dx.doi.org/10.1016/j.epsl.2012.10.024.
Plummer, L.N., Busenberg, E., 1982. The solubilities of calcite, aragonite and vaterite in CO_2–H_2O solutions between 0 and 90°C, and an evaluation of the aqueous model for the system $CaCO_3$–CO_2–H_2O. Geochim. Cosmochim. Acta 46, 1011–1040.
Quade, J., Eiler, J., Daeron, M., Achyuthan, H., 2013. The clumped isotope geothermometer in soil and paleosol carbonate. Geochim. Cosmochim. Acta 105, 92–107.
Retallack, G.J., 1994. The environmental factor approach to the interpretation of paleosols. In: Amundson, R., Harden, J., Singer, M. (Eds.), Factors of Soil Formation: A Fiftieth Anniversary Retrospective. Soil Science Society of America Special Publication.
Retallack, G.J., 2005. Pedogenic carbonate proxies for amount and seasonality of precipitation in paleosols. Geology 33, 333–336.
Rossi, B.E., 2004. Flora y vegetación de la Reserva de Biosfera de Nacuñán después de 25 años de clausura. Ph.D. thesis. La Universidad Nacional de Córdoba, Córdoba, Argentina.
Rossi, B.E., Villagra, P.E., 2003. Effects of *Prosopis flexuosa* on soil properties and the spatial pattern of understorey species in arid Argentina. J. Veg. Sci. 14, 543–550.
Royer, D.L., 1999. Depth to pedogenic carbonate horizon as a paleoprecipitation indicator? Geology 27, 1123–1126.
Schmidt, S., Hetzel, R., Mingoance, F., Ramos, V., 2011. Coseismic displacements and Holocene slip rates for two active thrust faults at the mountain front of the Andean Precordillera (~33°S). Tectonics 30, TC5011.
Silva, L.C.R., Giorgis, M.A., Anand, M., Enrico, L., Pérez-Harguineguy, N., Falczuk, V., Tieszen, L.L., Cabido, M., 2011. Plant Soil 349, 261–279.
Tobin, T.S., Schauer, A.J., Lewarch, E., 2011. Alteration of micromilled carbonate $\delta^{18}O$ during Kiel Device analysis. Rapid Commun. Mass Spectrom. 25, 2149–2152.
Villagra, P.E., Giordano, C., Alvarez, J.A., Cavagnaro, J.B., Guevara, A., Sartor, C., Passera, C., Greco, S., 2011. Ser planta en el desierto: estrategias de uso de agua y resistencia al estrés hídrico en el Monte Central de Argentina. Ecol. Austral. 21, 29–42.
Yang, W., Amundson, R., Trumbore, S., 1994. A model for soil $^{14}CO_2$ and its implications for using ^{14}C to date pedogenic carbonate. Geochim. Cosmochim. Acta 58, 393–399.
Zaarur, S., Affek, H.P., Brandon, M.T., 2013. A revised calibration of the clumped isotope thermometer. Earth Planet. Sci. Lett. 382, 47–57.